

Numerical analysis of phreatic levels in river embankments due to flood events

*Original*

Numerical analysis of phreatic levels in river embankments due to flood events / Butera, Ilaria; Cimaci, Marco; Tanda, Maria Giovanna. - In: JOURNAL OF HYDROLOGY. - ISSN 0022-1694. - STAMPA. - 590:(2020), pp. 1-9.  
[10.1016/j.jhydrol.2020.125382]

*Availability:*

This version is available at: 11583/2846013 since: 2020-10-06T16:12:59Z

*Publisher:*

Elsevier

*Published*

DOI:10.1016/j.jhydrol.2020.125382

*Terms of use:*

openAccess

This article is made available under terms and conditions as specified in the corresponding bibliographic description in the repository

*Publisher copyright*

(Article begins on next page)

1 Numerical analysis of phreatic levels in river embankments due to flood events

2 Ilenia Butera<sup>(a)</sup>, Marco Climaci<sup>(b)</sup> and Maria Giovanna Tanda<sup>(c)</sup>

3 (a) Associate professor, DIATI Politecnico di Torino, Corso Duca degli Abruzzi 24, 10129 Torino, email  
4 [ilaria.butera@polito.it](mailto:ilaria.butera@polito.it),

5 (b) Engineer, DIATI Politecnico di Torino, Corso Duca degli Abruzzi 24, 10129 Torino, email  
6 [marco@climaci.it](mailto:marco@climaci.it)

7 (c) Full professor, DIA Università degli Studi di Parma, Viale delle Scienze 181/A43124 Parma, email  
8 [mariagiovanna.tanda@unipr.it](mailto:mariagiovanna.tanda@unipr.it),

9

10

11

12 **Abstract**

13 A 2D saturated-unsaturated unsteady-flow numerical study has been carried out to analyze the behavior of  
14 levees stressed by flood events. The investigation has involved: i) simulation of the seepage process in a  
15 simplified levee over a long period of river flows; ii) the use of a synthetic design hydrograph to be utilized  
16 as an alternative to a long-term history of river stages and iii) the influence of the unsaturated parameters on  
17 the maximum saturation depth in the levee soil. The results of the analysis show that the statistical properties  
18 of the maximum annual piezometric levels are different from those of the corresponding river levels, and that  
19 the tested synthetic design-hydrograph is able to guarantee a well-balanced, conservative margin. The  
20 analysis shows that the role of the unsaturated zone is also very important. Furthermore, a comparison of the  
21 piezometric levels, computed by means of the numerical model, with those computed through simplified  
22 solutions, shows that the latter ones may not be conservative.

23

24 **Keywords:** Earthen levees; Flows through porous media; Levee piezometric levels; Modeling unsaturated  
25 zone; Synthetic Design Hydrograph

26

27

## 28 1 Introduction

29 River levees are important devices to control floods and protect the territory. The design of levees requires  
30 both geotechnical and hydraulic requirements to be taken into consideration For instance, the phreatic line  
31 should not cut the downstream side of an embankment, in order to avoid the triggering of erosive  
32 phenomena, which may reduce the water containment efficiency and compromise the stability of the  
33 embankment.

34 Many analysis have been carried out to understand the complex processes that levees undergo during flood  
35 events. For instance, fragility curves have been developed to consider the multiplicity of aspects that stress  
36 levees and cause their failure (hydraulic, geo-hydraulic and global static failures). Fragility curves are drawn  
37 up on the basis of physically-based and empirical process formalization (Vorogushyn et al., 2009) or  
38 experimental analyses (Hewett et al., 1987). Fragility curves constitute an important tool that can be used to  
39 support vulnerability and risk analyses (Camici et al., 2017; Mazzoleni et al., 2019), as, when combined with  
40 stochastic models of hydraulic loads, they allow the probability of levee failure to be computed. In this  
41 regard, the definition of the hydraulic loads for levee analysis is not a trivial matter, and it is a research topic  
42 of great interest: for instance, a copula-based model, which considers both the peak flow discharge and flow  
43 duration, has been proposed for the estimation of the structural residual hazard (Balistrocchi et al., 2019) and  
44 the use of a Synthetic Design-Hydrograph (SDH) has been suggested for levee design purposes (Butera and  
45 Tanda, 2006).

46 When dealing with river levees, one of the most important aspects is the identification of the phreatic line.

47 To this aim, geometric and empirical criteria were developed in the past to identify the location of the  
48 phreatic line (e.g. Shaffernak, 1917; Casagrande, 1940; Kozeny, 1931; USACE, 1993).

49 Apart from resorting to geometric and empirical criteria, accurate and site specific descriptions of the  
50 phreatic line location can also be obtained by means of numerical models. The currently used numerical  
51 models, in fact, allow seepage phenomena through a levee to be simulated by taking into account the  
52 geometry of the embankment, the soil properties and appropriate boundary and initial conditions. The  
53 reliability of the numerical results depend on an accurate definition of the hydraulic head boundary condition  
54 and the adoption of adequate soil parameters. It is usual practice to consider steady-state conditions in these  
55 models, assuming a water level that is constant over time at the river side of the embankment and equal to

56 the river stage of the discharge value of the design return period. However, a flood event produces an  
57 unsteady flow, and a phreatic line that changes over time. The design of an embankment under steady  
58 conditions can lead to an oversizing of the embankment (and therefore to a non-economic design, USACE,  
59 2013; Butera and Tanda 2006) and, even more worrying, cannot account for possible instabilities due to  
60 changes in the water level in the river (e.g. Rinaldi et al., 2004; Kwang Seok Yoon, 2005; Stark et al., 2014;  
61 Jafari et al., 2019). Such instabilities in some cases can be acceptable, if controlled, as stated in Lupiano et al.  
62 (2020) where dams have been designed with backfilling, through the implementation of a steady-state  
63 numerical model, to ensure that the failure occurs at an appropriate water level.

64 A transient analysis is of fundamental importance to assess slope stability, and a fully coupled unsteady  
65 flow-mechanics analysis (e.g. Pinyal et al., 2008; Voltz et al., 2017), in which attention is paid to the  
66 composition of the soil and to the soil parameter values (e.g. Elkholy et al., 2015), is desirable. The  
67 drawdown effect on the riverside can in fact be quite risky (e.g. Mitchell and Hunt, 1985), and an analysis  
68 under steady state conditions is not able to handle such a case.

69 The use of numerical models under unsteady conditions allows not only the modifications in time of the  
70 phreatic line to be understood and taken into account, but also the role of the hydraulic content in the  
71 unsaturated zone of the levee. The role of the unsaturated zone and its effect on the piezometric levels  
72 reached during flood events is a topic which, to the best of the Authors' knowledge, has received very little  
73 attention.

74 Traditional approaches that deal with the issue of the piezometric levels reached in a levee and the problem  
75 of levee dimensions under unsteady conditions did not consider the impact of the unsaturated zone, that is,  
76 they considered that the soil above the piezometric surface was completely dry. Supino (1955) and Marchi  
77 (1957) suggested relatively simple solutions to compute, under a few hypotheses, the location of the phreatic  
78 line in unsteady conditions. It should be mentioned that such semi-analytical solutions are valid for the  
79 linearization of the flow equation and assume Dupuit's hypothesis. Giugni and Fontana (1999) then extended  
80 the work of Marchi to a nonlinear flow equation and removed Dupuit's assumption.

81 The present work pertains to the analyses of the seepage process in a levee under unsteady conditions, with  
82 particular attention being paid to the maximum annual piezometric levels reached in the levee. A saturated-  
83 unsaturated numerical model has been used and the analysis concerns the following three aspects: 1) the

84 statistical characterization of the piezometric levels reached in the levee; 2) the use of synthetic hydrographs  
85 for the analysis of the seepage in the levee; 3) the sensitivity of the saturated-unsaturated dynamics in the  
86 levee to the unsaturated soil parameters, i.e. the impact of soil retention and the relative hydraulic  
87 conductivity curves.

88 The analysis has been carried out at a real site: the Pontelagoscuro Po River section (Ferrara, Italy). Public  
89 Agencies, devoted to hydrological surveying and to the planning and management of the Po River, have  
90 recorded the river water levels in Pontelagoscuro for many years. The daily water levels and hourly  
91 observations during flood events are in fact available for this hydrograph station for the years 1951 to 2016.  
92 Furthermore, synthetic hydrographs are also available for the Pontelagoscuro section: Maione et al. (2003)  
93 developed special design hydrographs (SDH – Synthetic Design-Hydrograph) for Po River sections that are  
94 useful for numerical simulations of flood routing; these SDHs can be used for the prediction of the  
95 maximum water levels while taking into account the storage due to the inundation of the floodplains. The  
96 possibility of deriving SDHs from a regional analysis (e.g. Tomirotti and Mignosa, 2017), without the  
97 necessity of historical records, suggests testing the suitability of SDHs for levees design.

98 The manuscript is organized as follows: a brief description of the mathematical statement of the problem is  
99 presented, and this is followed by a description of the data and the numerical model. The first part of the  
100 analysis concerns a statistical characterization of the piezometric level in the levee, which is followed by the  
101 evaluation of the impact of the use of SDHs for the hydraulic load. The analysis concludes with the treatment  
102 of the role of the unsaturated zone. The work is completed with a discussion of the results and some  
103 conclusions.

104

## 105 2 Mathematical statement of the problem

106 Darcy's law and continuity equations govern seepage phenomena through an embankment: inserting Darcy's  
107 law into the continuity equation, for a homogeneous and variously saturated medium, one obtains the  
108 following equation:

$$109 \quad \frac{\partial}{\partial x} \left( K(\theta_w) \frac{\partial h}{\partial x} \right) + \frac{\partial}{\partial y} \left( K(\theta_w) \frac{\partial h}{\partial y} \right) + \frac{\partial}{\partial z} \left( K(\theta_w) \frac{\partial h}{\partial z} \right) = S_0 \frac{\partial h}{\partial t} \quad (1)$$

110 where  $h$  is the piezometric head inside the levee, and  $\theta_w$ ,  $K$  and  $S_0$  are the water content, the hydraulic  
 111 conductivity and the specific storage coefficient of the soil, respectively. Eq. (1) is completed with the  
 112 relations that describe the link between the piezometric height and the water content of the soil (i.e. the  
 113 retention curve  $h=h(\theta_w)$ ) and the relationship between the hydraulic conductivity and the water content of the  
 114 porous matrix ( $K=K(\theta_w)$ ).

115 The Van Genuchten model (Van Genuchten, 1980) for unsaturated soil has been used in the present work:

$$116 \quad \theta_e = \left[ 1 + (\alpha \cdot \psi)^n \right]^{-m} \quad (2)$$

117 where the effective water content,  $\theta_e$ , is related to the irreducible water content,  $\theta_r$ , and to porosity  $n$  through  
 118 the following equation:

$$119 \quad \theta_e = \frac{\theta_w - \theta_r}{n - \theta_r} \quad (3)$$

120 The symbol  $\psi$  in (2) stands for the suction in the ground (or capillary head), which is defined as the opposite  
 121 of the piezometric height:

$$122 \quad \psi = -\frac{p_w}{\gamma_w} \quad h = z + \frac{p_w}{\gamma_w} = z - \psi \quad (4)$$

123 In expression (4),  $p_w$  and  $\gamma_w$  are the pressure and the specific weight of the water, respectively. The  
 124 coefficients  $\alpha$  and  $n$  in (2) have to be determined experimentally, while

$$125 \quad m = 1 - \frac{1}{n} \quad (5)$$

126 The relationship between the hydraulic conductivity and the water content is defined by introducing the  
 127 relative hydraulic conductivity coefficient,  $K_{rr}$ , which represents the ratio between the hydraulic conductivity  
 128 of the soil of a generic water content with respect to the saturated hydraulic conductivity:

$$129 \quad K_r = \frac{K(\theta_w)}{K_{sat}} \quad (6)$$

130 Van Genuchten stated (1980) that:

131

$$K_r = \theta_e^{1/2} \left[ 1 - \left( 1 - \theta_e^{1/m} \right)^m \right]^2. \quad (7)$$

132 The boundary and initial conditions define the solution of the differential equation (1).

133 The 3D problem defined by relations (1) to (7) is complex, and some simplifications of the problem were  
 134 proposed in the past that allowed analytical or semi-analytical solutions to be obtained. These solutions can  
 135 capture the main features of the phenomena, but do not consider, for instance, the role of the unsaturated  
 136 zone. In this article, we refer, in some of the comparisons, to the semi-analytical model of Marchi (1957), as  
 137 already used by Butera and Tanda (2006).

139

### 140 3 The data and their processing

141 The case study deals with the Pontelagoscuro section of the Po River (Italy). The catchment area of the basin  
 142 is 70091 km<sup>2</sup>. The considered data pertain to the water levels observed in the 1 January 1951 to 31 December  
 143 2016 period. The water level is recorded and published daily in yearbooks, although, upon request, hourly  
 144 step data can be supplied.

145 Some morphological changes occurred in the river during the examined period; in particular, a lowering of  
 146 the river bed was detected (Marchetti, 2002) which caused modifications of the geometry of the river section  
 147 and, for this reason, the observed water levels cannot be considered to constitute a homogeneous time series.  
 148 In order to obtain results with the usual statistical analysis tools for stationary time series, we modified the  
 149 observed water level data with the procedure described hereafter.

150 The stage data were converted into discharge data using the rating curve considered reliable during the  
 151 observation period (96 relations in the considered period) and all the obtained discharge values were then  
 152 back-converted to stage values using the same rating curve, that is, the 1982 rating curve, which was chosen  
 153 arbitrarily. The thus obtained water levels were interpolated to obtain a one-hour time step sequence to use in  
 154 the numerical simulations. The achieved dataset may be considered as homogeneous, and is referred to, in  
 155 the following, as the rearranged historical stage time series (rearranged stage history –RSH– in short).

156 Figure 1 shows the frequency of occurrence of the stage values in the RSH, which was obtained by  
 157 processing the 66 years of rearranged data: the abscissa value for a given stage in the ordinate axis describes  
 158 the number of days for which that stage value is exceeded in an average year. The line depicted in Fig. 1 is

159 the stage-duration curve: the minimum value is 1.01 m a.s.l., the maximum is 12.11 m a.s.l., the median  
160 value is 3.30 m a.s.l and the mean value is 3.66 m a.s.l..

161 *HERE FIGURE 1*

162 The synthetic design hydrographs (in short SDH) were obtained for the same Pontelagoscuo section  
163 (Maione et al., 2003), by processing the data available for different return periods  $-T_r-$  ( $T_r = 2, 5, 10, 20, 50,$   
164  $100, 200$  and  $500$  years). The duration of the hydrographs was set equal to 953 hours, which corresponds to  
165 the 95% percentile of the durations of the hydrological events whose water levels are higher than the level  
166 that corresponds to the 80% percentile of the historical water level series. These percentile values were set so  
167 that the duration of the SDHs was representative of the flood event durations. The SDHs were transformed,  
168 through the 1982 rating curve, into time patterns of the water levels, and Synthetic Design Level Diagrams,  
169 in short SDLs, were thus obtained (Butera and Tanda, 2006). The obtained SDHs and SDLs are shown in  
170 Fig. 2 for the 2016 updated observations.

171 The RHS and the SDLs were used as boundary conditions for the upstream edge of the levee, i.e. the river  
172 side, both in the semi-analytical model and in the numerical one. The legend of the different curves in Fig.  
173 2b reports the return period of the SDH that was used to create the SDL, although, in principle, it cannot be  
174 assumed as the return period of the SDL.

175 *HERE FIGURE 2*

176

177

## 178 4 Numerical model

179 The FEMWATER code (Lin et al., 1997) was used for the numerical model of the seepage. A rectangular-  
180 shaped prism model was built with the dimensions and physical parameters defined according to the main  
181 characteristics of the Pontelagoscuo levee, although a greatly simplified geometry was assumed (Fig. 3).

182 The dimensions of the model in the horizontal plane are: 500m in the  $x$  direction, orthogonal to the river, and  
183 1m in the  $y$  direction parallel to the river. The extension of the model in the  $x$  direction was considered long  
184 enough to reduce the impact of the downstream boundary condition (Fig. 3). Only one column of elements,  
185 whose size was fixed at 1m, was considered in the  $y$  direction; since the surfaces of the vertical planes at



186  $y=0\text{m}$  and  $y=1\text{m}$  were set as impervious, the thus built 3D model behaves like a 2D model in the vertical  
187 plane.

188 *HERE FIGURE 3*

189 The vertical dimension of the model is 66.38m. The model elements change size along the  $x$  and  $z$  locations:  
190 they are smaller where higher variations of the piezometric head can be expected, that is, upstream close to  
191 the river, and in the upper zone of the model where the phreatic line moves in response to the transient water  
192 levels in the river. The side of the elements varies between 1m and 7m along the  $x$  direction and between 1m  
193 and 5m along the  $z$  direction.

194 The water levels in the embankment were analyzed at 10 sections at different distances from the upstream  
195 face (riverside); their locations are summarized in Table 1.

196 *HERE TABLE 1*

197 As far as the boundary conditions are concerned, the bottom of the model is a horizontal and impervious  
198 plane located at -50 m a.s.l, the RHS, or alternatively the SLDs, represent the boundary condition at the  
199 riverside, while a constant total head with a value equal to that of the initial condition was given to the  
200 downstream boundary. As mentioned above, impervious boundary conditions were adopted on the vertical  
201 planes that delimit the model in the  $y$  direction. Moreover, the upper horizontal plane of the model was  
202 assumed impervious, i.e. no recharge or evaporation was considered possible through the soil surface during  
203 the simulations. A static condition, whose value influences the distribution of the humidity in the unsaturated  
204 zone, was assumed for the initial conditions over the entire domain.

205 The initial condition was set equal to the first value of the water level series (i.e. 3.78 m a.s.l., January 1<sup>st</sup>  
206 1951) in the RHS simulations, so that the initial depth of the aquifer was set equal to 53.78 m. Preliminary  
207 runs, showed that the memory of the initial condition in the analysis of the RHS (66 years long) is limited:  
208 differences in the initial condition equal to 2.7 m after 2.5 months of simulation resulted in maximum  
209 changes of 0.18 m.

210 According to the technical reports on the Pontelagoscuoro levees (e.g. SISMAPO project, 2015), the soil in  
211 the levee was considered as a sandy silt with a total porosity and hydraulic conductivity equal to 0.406 and  
212  $5 \cdot 10^{-6}$  m/s, respectively.

213 Van Genuchten relations were used to describe the physical properties of the unsaturated soil and, due to the  
214 absence of specific investigations, the relative parameters were defined according to the procedure  
215 introduced by Sleep (2011). The residual water content was assumed equal to 10% of the total porosity and  
216 the parameters of equations (2) and (3) were estimated considering different humidity conditions of the soil.  
217 Since the value of these parameters changes as a function of the wetting or drying conditions, five different  
218 conditions, all-referring to sandy silt soil, were considered, and the estimated parameters are shown in Table  
219 2. The “Average wetting condition (AW)” and the “Average drying condition (AD)” refer to the values  
220 averaged over different experiments on sandy silt samples under wetting and drying conditions, respectively.  
221 The “Wetting Boundary 90 % confidence condition (WB90)” values are the parameter values of the lower  
222 extreme of the 90% confidence interval for wetting condition samples, while those of the “Drying Boundary  
223 90% confidence (DB90) condition” are the parameter values of the upper extreme of the 90% confidence  
224 interval for drying condition samples. The parameter values of the Average Wetting-Drying (AW-D)  
225 condition are the average values of the Average Wetting condition (AW) and the Average Drying (AD)  
226 condition. Figure 4 shows the characteristic curves of the unsaturated soil for the considered conditions;  
227 reference can be made to Sleep (2011) for more details.

228 *HERE FIGURE 4*

229 *HERE TABLE 2*

230 A Matlab post processor code was written to identify the location of the phreatic line at each monitoring  
231 section of the levee (i.e. where the water pressure is equal to the atmospheric pressure). Given the curvature  
232 of the streamlines, the pressure distribution cannot be considered hydrostatic in the x-z vertical plane and the  
233 location of the piezometric surface therefore cannot be computed as being equivalent to the piezometric head  
234 at the computation point. The elevation of the piezometric surface in the levee was computed at each section  
235 by means of a bi-linear interpolation of the pressure field, which in turn was determined by means of the  
236 Femwater code for the area where the soil conditions change from saturated to unsaturated.

237

## 238 5 Characterization of the levee levels stressed by the RHS

239 A statistical analysis of the maximum annual water levels reached in the sections considered in Table 1 for  
240 the simulation of the 66-year river stage has been carried out. The initial condition was hypothesized as a

241 horizontal piezometric surface at 3.78 m a.s.l., that is, corresponding to the first datum value of the historical  
242 water levels, which is equivalent to the water level that is reached for 128 days throughout the average year.  
243 The unsaturated soil was described using the average wetting-drying condition (Table 2); the impact of the  
244 parameter values on the unsaturated zone is discussed in the following section.

245 As a first step of the analysis, the return periods of the annual maximum phreatic levels, in the sections listed  
246 in Table 1, were compared with the return periods of the annual maximum levels in the river for each year of  
247 the RHS simulation.

248 The maximum annual approach is able to compute the return period of the annual maximum phreatic levels  
249 in the levee and the river water levels obtained from the RHS simulation. The maximum value for each year  
250 was found for each levee section and for the river; the thus obtained series (66 data for each section) were  
251 then processed to identify the statistical distribution that best fitted the data. Six distributions were tested  
252 (normal, log-normal, gamma, GEV, the extreme value and the exponential one). It emerged that, according  
253 to the Bayesian information criterion, the distribution that best fitted the data in all the sections was the  
254 normal one.

255 Using the parameters of the best-fit statistical distribution, the return period of each annual maximum value  
256 was then computed and compared with the return period of the annual maximum water level in the river for  
257 the same year. Although it was possible that the values did not refer to the same flood event, any diversity  
258 that can be observed in Fig. 5 highlights that the stress degree of a flood event for a levee may have been  
259 different from that of the river.

260 *HERE FIGURE 5*

261  
262 Figure 5 shows the results of the analysis: as can be seen, markers located at the 45°-degree line mean that,  
263 in a certain year, the river and the levee section underwent events of the same severity. Markers located  
264 under the 45°-degree line show that the flood events had been more severe for the river than for the levee;  
265 the opposite holds for markers located above the 45°-degree line. In the latter case, the levee is stressed even  
266 when the levels in the river are not very high. This is due to the nonlinearity of the process that relates the  
267 river levels and the seepage in the levee. In fact, not only does the maximum value of the hydrographs

268 influence the piezometric levels in the levee, but also their shapes (i.e. the duration of the water height in the  
269 river that can be linked to the floodwater volume).

270 These results show the importance of testing the use of SDLDs for the design of a levee under unsteady  
271 conditions: SDLDs are, in fact, built considering not only the maximum discharge values, but also the flood  
272 volumes.

273

## 274 6 Characterization of the phreatic levels in the levee stressed by SDLDs

275 In order to test the suitability of the SDLDs to represents the excitations applied to the levee and then to  
276 obtain design information, the SDLD obtained from an SDH with a return period of 200 years was applied as  
277 a boundary condition at the riverside. An SDH with a return period equal to 200 years was used because this  
278 is the main reference value prescribed by Italian Public Agencies devoted to the planning and management  
279 of the Po River (e.g. Autorità di bacino del fiume Po, 2010). Such a diagram is here referred to as  $SDLD_{\ell 200}$   
280 (SDLD labeled for 200 years).

281 The results of the computations were compared with the phreatic line level obtained for each levee section by  
282 means of the previously mentioned statistical inference with a return period of 200 years (Fig. 6).

283 As can be seen in Fig. 2b, the used  $SDLD_{\ell 200}$  has a high initial value of 7.31 m a.s.l. When a level of 7.31 m  
284 a.s.l. is assumed as the initial condition for the piezometric surface in the levee, high levels were reached in  
285 the levee during a flood. In fact, much of the levee is under saturated conditions before the beginning of a  
286 flood (for  $z < 7.31$  m a.s.l.) and the storage capacity of the levee is reduced.

287 In order to evaluate the impact of the initial level of the horizontal phreatic surface (which also influences the  
288 initial water content in the unsaturated zone), an analysis was performed considering different initial  
289 conditions, and the results are shown in Fig. 6. Five values, which were obtained by dividing the difference  
290 between the first datum of the  $SDLD_{\ell 200}$  (7.31 m a.s.l.) and the first datum of the RHS (3.78 m a.s.l.) into  
291 five parts, were chosen as the initial condition. In terms of percentiles of the river water level set, the 3.78m  
292 hydraulic level corresponds to the 68% percentile, while 7.31 m a.s.l corresponds to the 97.35 % percentile.  
293 It should be pointed out that a different initial level in the aquifer from the starting value of the river

294 hydrograph causes an abrupt change in the river side, which may induce numerical instabilities; reduced time  
295 steps were therefore adopted to avoid simulation problems.

296 Figure 6 shows the hydraulic levels reached in the levee sections when  $SDL D_{\ell 200}$ , which was derived from  
297 the SDH with a return period equal to 200 years, is used and different initial piezometric levels are  
298 considered. As expected, the differences in the curves are remarkable, and this underlines that the initial  
299 aquifer conditions, which in general are not so well defined, play an important role in the evolution of the  
300 phreatic line.

301 *HERE FIGURE 6*

302 The phreatic levels obtained after the inference of the probability distribution of the phreatic levels are  
303 compared, in the same figure, with the hydraulic level for a return period equal to 200 years, as computed  
304 from the statistical analysis of the maximum annual values. It can be seen that the use of SDL Ds, obtained  
305 from the SDHs of the return period equal to 200 years, is conservative for all the sections when the initial  
306 condition of the level is greater than 4.66 m a.s.l, that is, for the 82% percentile of the RHS stages.  
307 This result seems to be justified by the fact that the phreatic line in the embankment changes quite slowly  
308 after a flood and, as a result, it is necessary to adopt moderate initial high water level conditions in the levee  
309 domain to simulate severe excitations for the 200 year return period.

310

## 311 7 The impact of the unsaturated zone parameters

312 The possibility of modeling the unsaturated zone is one of the main reasons for using numerical models  
313 instead of semi-analytical solutions. The Femwater code does not reproduce the characteristic hysteresis of  
314 the retention curve, and only one curve in Fig. 3 can be used at a time.

315 In order to test the impact of the parameters that characterize the unsaturated zone, the numerical model was  
316 run with the different sets of parameters listed in Table 2. In this analysis, the  $SDL D_{\ell 200}$  obtained from the  
317 SDH for a return period equal to 200 years was used as the riverside condition and the initial level of the  
318 phreatic surface was set equal to the first level of the SDL D series, i.e. 7.31 m a.s.l. The following  
319 dimensionless coefficient, which was named infiltration ratio (*IR*), was introduced to analyze the behavior of  
320 the water levels in the levee:

$$IR(x,t) = \frac{h(x,t) - h_{il}}{h_{\max}(x=0) - h_{il}} \quad (8)$$

321

322 where  $h(x,t)$  in (8) is the water level at time  $t$  and distance  $x$  from the levee riverside,  $h_{il}$  is the initial level at  
 323 distance  $x$  and  $h_{\max}(x=0)$  is the maximum level reached in the river. The  $IR(x,t)$  parameter varies from 0 to 1:  
 324 a value of  $IR$  close to zero means that the flood event in the river does not affect the piezometric level in the  
 325 levee sections. Higher values of  $IR$  indicate a prompt response of the levee aquifer to changes in the water  
 326 level in the river.

327 Panels a) to d) in Fig. 7 show the infiltration ratio values as a function of time at different distances from the  
 328 riverside. The results obtained from the numerical simulations using the parameters listed in Table 2 are  
 329 shown together with the levels computed with the semi-analytical solution introduced by Marchi (1957) in  
 330 each panel. It should be pointed out that, when adopting the Marchi solution, the ratio between the rise in the  
 331 river levels and the initial thickness of the levee aquifer should be less than 0.25 in order to guarantee the  
 332 reliability of the linearization process.

333

*HERE FIGURE 7*

334 The piezometric surface levels decrease in all the sections as the  $\alpha$  parameter in eq. (2) increases. Increasing  
 335 the  $\alpha$  value, for a given suction value (see Fig. 4), means that the unsaturated soil has a low level of humidity  
 336 and, as a result, the soil has a greater storage capacity, and the piezometric levels of the levee therefore  
 337 increase less than in the case of drying conditions (a smaller  $\alpha$  value). If the distance from the river is  
 338 increased, the results obtained through the semi-analytical approach (SA in the legend in Fig. 7) are below  
 339 those obtained by means of numerical modeling. This result can be explained by considering that the semi-  
 340 analytical approach does not take into account the presence of humidity above the piezometric surface, and  
 341 thus relies on a greater water storage capacity in the soil pores. The semi-analytical model solution for the  
 342 levee sections close to the river is not always below the ones provided by the numeric model: the semi-  
 343 analytical solution, obtained under Dupuit's hypothesis, is less accurate close to the river because of the non-  
 344 negligible vertical components of the flow field.

345 Table 3 and Fig. 8 show the maximum levels reached in each monitoring section obtained using the semi-  
 346 analytical solution and the numerical model with different  $\alpha$  values. Remarkable differences can be noticed

347 when different values of the  $\alpha$  coefficients are used, and the semi-analytical solution underestimates the  
348 piezometric surface levels in most of the tested conditions.

349 *HERE TABLE 3*

350 Figure 8 and Table 3 also point out the role of the water content in the unsaturated zone when the flood wave  
351 passes in the river. If the levee is in drying conditions, because a previous flood event has recently occurred,  
352 the levee aquifer levels will be higher than those that would be reached if the levee were under wetting  
353 conditions. It is in fact known, from field experience, that a levee can collapse in the case of multiple peak  
354 floods, when a flood peak occurs, even if it is lower than the previous one, because the levee has a higher  
355 initial water content.

356

## 357 8 Conclusions

358 In this work, a two-dimensional numerical model has been adopted to analyze the water levels in a levee.  
359 The analysis mainly concerned three aspects: i) the statistical characterization of the water levels in the levee  
360 compared to that of the river, ii) the use of synthetic design level diagrams (SDLs) derived from synthetic  
361 design hydrographs (SDH) and iii) the role of the unsaturated zone in the piezometric levels of the levee.  
362 In order to deal with the first issue, a historical water level series, rearranged to obtain an acceptable  
363 homogeneity level, was considered as the riverside condition. The statistical analysis of the annual maximum  
364 levels, reached at different distances from the riverside, showed that the maximum return period of the  
365 annual maximum of the piezometric levels in the levee is different from that of the river levels. This result  
366 confirms that the stresses in the levee may in part be due to factors other than the maximum water level in  
367 the river.

368 The use of SDHs, transformed into SDLs (Synthetic Design Level Diagrams), has proved to be useful to  
369 identify the piezometric surface. The obtained results have shown that the use of the first datum of the  
370 SDLs as the initial condition is appropriate, even though it may appear too precautionary. It has also been  
371 shown that  $SDL_{/200}$ , labeled for a 200-year return period, can be used to estimate, with a certain  
372 approximation, the piezometric levels of the same return period obtained after statistical inference of the  
373 values resulting from the simulation of the historical time series of the river levels. Since SDHs can be

374 derived from a regional analysis (Maione et al., 2003; Tomirotti and Mignosa, 2017), without the necessity  
375 of historical records, it is the Authors' opinion that SDDL represents an alternative levee design tool. It  
376 produces results that are well-balanced between the traditional static design, with the maximum river stage  
377 under steady conditions, and those of an analysis under unsteady conditions with a historical time series of  
378 the river stages.

379 It has emerged, from the sensitivity analysis of Van Genuchten's  $\alpha$  parameter, that this parameter has a great  
380 impact on the maximum piezometric levels. A smaller  $\alpha$  value implies higher piezometric levels.

381 Finally, it has been found that simplified semi-analytical models are not reliable close to the riverside  
382 (because Dupuit's formula does not apply) or at a distance from the riverside (because the role of the  
383 unsaturated zone is neglected); moreover, their results are often not conservative.

384 An analysis under transient conditions will be carried out through an integrated hydraulic-geotechnical  
385 approach as a future development of the present research, in order to establish the best precautionary design  
386 conditions for the stability of the levee which do not lead to an oversized design.

387

## 388 Acknowledgements

389 The Authors would like to thank the Inter-regional Agency for the river Po (AIPO) for providing the data

390

## 391 Funding

392 This research was partially supported by the Ministry of the Environment and the Protection of the Territory  
393 and the Sea, DILEMMA (Imaging, Modeling, Monitoring and Design of Earthen Levees) project.

394

395



396 **References**

- 397 Autorità di bacino del fiume Po, 2015. La verifica sismica delle arginature, SISMAPO Project. Final report
- 398 Autorità di bacino del fiume Po, 2010. Variante al PAI. Relazione Tecnica, allegato alla delib. 7 del 21  
399 dicembre 2010.
- 400 Balistrocchi, M., Moretti G., Orlandini S., Ranzi R., 2019. Copula-based modeling of earthen levee breach  
401 due to overtopping, *Advances in water resources*, 134.  
402 <https://doi.org/10.1016/j.advwatres.2019.103433>
- 403 Butera, I., Tanda, M. G., 2006. Analysing river bank seepage with a synthetic design hydrograph, *Water*  
404 *Management*, 119-127. <https://doi.org/10.1680/wama.2006.159.2.119>
- 405 Camici, S., Barbetta, S., Moramarco T., 2017. Levee body vulnerability to seepage: the case study of the  
406 levee failure along the Foenna stream on 1 January 2006 (central Italy), *Journal of flood risk*  
407 *management*, 10, 314-325. DOI: 10.1111/jfr3.12137
- 408 Casagrande A., 1940. Seepage through the dams. Contribution to soil mechanics 1925–1940. Boston: Boston  
409 Society of Civil Engineers.
- 410 D’Oria, M., Maranzoni, A., Mazzoleni M., 2019. Probabilistic Assessment of Flood Hazard due to Levee  
411 Breaches Using Fragility Functions, *Water Resources Research*.  
412 <https://doi.org/10.1029/2019WR025369>
- 413 Elkholy, M., Sharif, Y. A., Chaudhry, M.H., Imran, J., 2015. Effect of soil composition on piping erosion of  
414 earthen levees., *Journal of Hydraulic Research*, 53, 478-487.  
415 <https://doi.org/10.1080/00221686.2015.1026951>
- 416 Giugni, M., Fontana, N., 1999. Sulla determinazione della linea di infiltrazione all’interno di un argine  
417 fluviale, *L’Acqua* 5/1999, ISSN 1125-1255 (in italian).
- 418 Hewett, H. , Boorman, L. , Bramley, M., 1987. Design of Reinforced Grass Waterways. Construction  
419 Industry Research and Information Association, London, UK .

- 420 Kozeny J., 1931. Grundwasserbewegung bei freiem Spiegel, Fluss und Kanalversickerung, Wasserkraft und  
421 Wasserrwirtschaft, no 3.
- 422 Kwang S. Y., 2005. Failure Causes and Design Methods of River Levees, *Second Joint Seminar between*  
423 *IWHR and KICT*, July 11-15, 2005, Bijing, Chine.
- 424 Jafari, N.H., Cadigan, J.A., Stark, T.D., Woodward, M.L., 2019. Phreatic surface mitigation through an  
425 unsaturated levee embankment, *J. of Getechnical and Geoenvironmental Engineering*, 145:  
426 05019010
- 427 Lin, H.C.J., Richards, D.R., Talbot, C.A., Yeh, G.T., Cheng J.R., Cheng H.P., Jones N.L., 1997.  
428 FEMWATER: A three-dimensional finite element computer model for simulating density-dependent  
429 flow and transport in variable saturated media. Technical Report CHL-97-12. U.S. Army Corps of  
430 Engineers, Waterways Exp. Station. Vicksburg. Mississipi. USA.
- 431 Lupiano, V., Chidichimo, F., Machado, G., Catelan, P., Molina, L., Calidonna, C.R., Straface, S., Crisci,  
432 G.M., Di Gregorio, S., 2020. From examination of natural events to a proposal for risk mitigation of  
433 lahars by a cellular-automata methodology: a case study for Vascún valley, Ecuador. *Natural*  
434 *Hazards and Earth Systems Science (NHES)*, 20, 1-20 <https://doi.org/10.5194/nhess-20-1-2020>
- 435 Maione, U., Mignosa, P., Tomirotti, M., 2003. Regional estimation of syntetic design hydrographs, *Intl. J.*  
436 *River Basin Management*, 1, 151-163. doi:10.1080/15715124.2003.9635202
- 437 Marchetti, M., 2002. Environmental changes in central Po Plain (northern Italy) due to fluvial modifications  
438 and anthropocenic activites. *Geomorphology*, 44, 361-373 [https://doi.org/10.1016/S0169-](https://doi.org/10.1016/S0169-555X(01)00183-0)  
439 [555X\(01\)00183-0](https://doi.org/10.1016/S0169-555X(01)00183-0)
- 440 Marchi, E., 1957. Un criterio per la verifica alla filtrazione delle arginature in terra, *Giornale del Genio*  
441 *Civile*. (in italian)
- 442 Mitchell, P.H., Hunt B., 1985. Unsteady groundwater drawdown in embankments. *Journal of Hydraulic*  
443 *Research*. 23, 241-254.

- 444 Pinyol, N. M., Alonso, E. E., Olivella S., 2008. Rapid drawdown in slopes and embankments, *Water Resour.*  
445 *Res.*, 44, W00D03, doi:10.1029/2007WR006525.
- 446 Rinaldi, M., Casagli, N., Dapprto, S., Gargini, A., 2004. Monitoring and modelling of pore water pressure  
447 changes and riverbank stability during flow events, *Earth Surface Processes and Landforms* 29, 237-  
448 254 <https://doi-org.ezproxy.biblio.polito.it/10.1002/esp.1042>
- 449 Schafferank, F., 1917. Über die Standicherheit durchlaessiger geschuetteter Dämme, *Allge, Eauzeitung*.
- 450 Sleep, M. D., 2011. *Analysis of Transient Seepage Through Levees*. Blacksburg, VA.
- 451 Stark, T.D., Jafari, N.H., Leopold, A.L., Brandon T.L., 2014. Soil compressibility in transient unsaturated  
452 seepage analyses, *Canadian Geotech. J.* 51, 858-868 <https://doi.org/10.1139/cgj-2013-0255>
- 453 Supino, G., 1955. La linea di filtrazione negli argini e nelle dighe in terra. Calcolo di stabilità per le  
454 arginature fluviali, *Atti del V Convegno regionale dell'Ass. Idrotecnica Italiana* (in italian).
- 455 Tomirotti, M., Mignosa, P., 2017. A methodology to derive Synthetic Design Hydrographs for river flood  
456 management, *Journal of Hydrology*. 555. 10.1016/j.jhydrol.2017.10.036.
- 457 USACE., 1993. Seepage analysis and control for dams. E.M. 1110-2-1901.
- 458 USACE., 2013. The international levee handbook. CIRIA
- 459 Van Genuchten, M., 1980. A closed-form equation for predicting the hydraulic conductivity of unsaturated  
460 soils. *Soil Sci. Soc. Am.J*, 44, 892-898.
- 461 Volz, C., Frank, P.J., Vetsch, D.F., Hager, W.H., Boes, R.M., 2017. Numerical embankment breach  
462 modelling including seepage flow effects. *Journal of Hydraulic Research*, 55, 480-490.  
463 <https://doi.org/10.1080/00221686.2016.1276104>
- 464 Vorogushyn, S., Merz, B., Apel, H., 2009. Development of dike fragility curves for piping and micro-  
465 instability breach mechanisms. *Nat. Hazard Earth Syst. Sci.* 9 (4), 1383–1401.  
466 <https://doi.org/10.5194/nhess-9-1383-2009> .

467

Figure 1  
[Click here to download high resolution image](#)

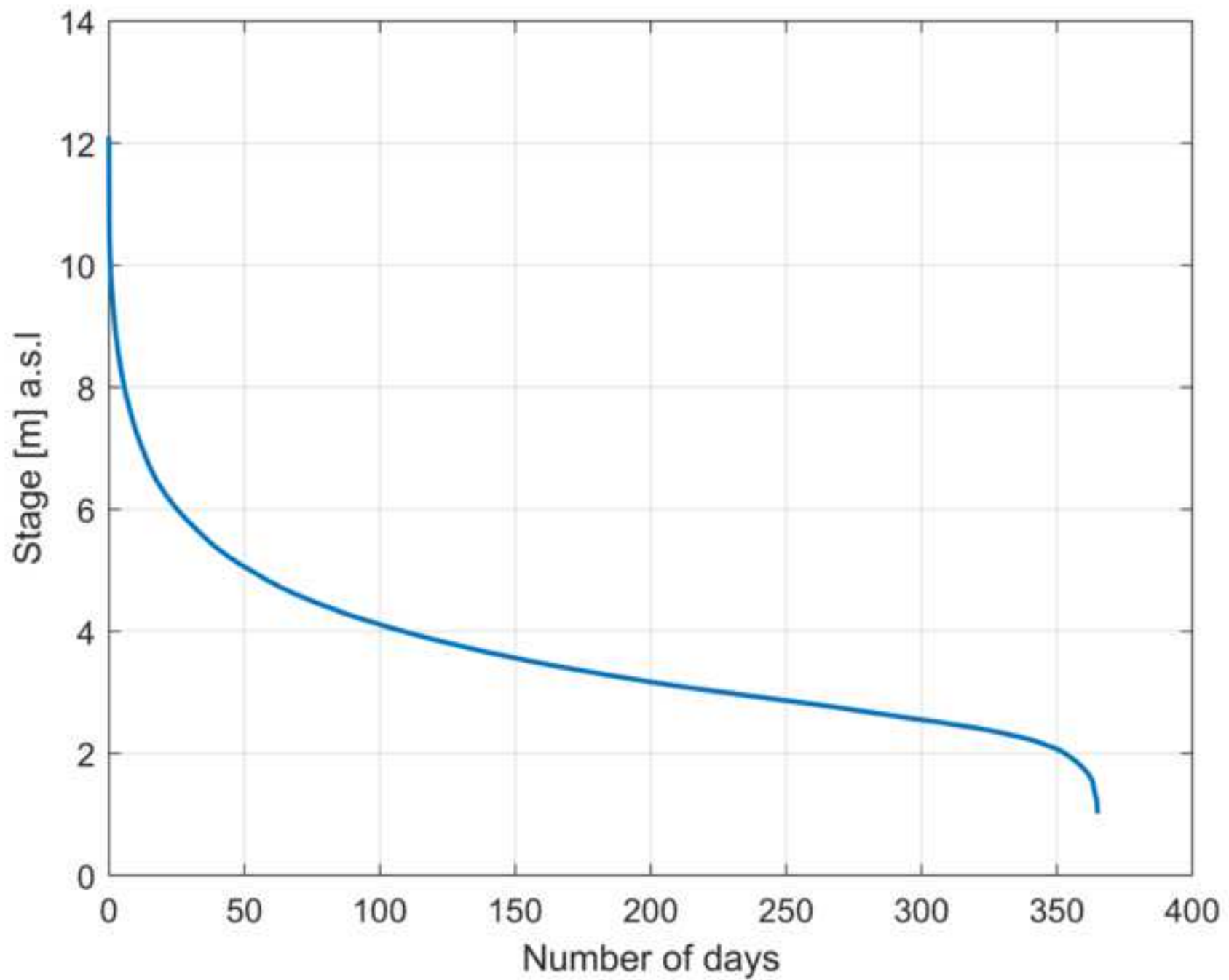


Figure 2a  
[Click here to download high resolution image](#)

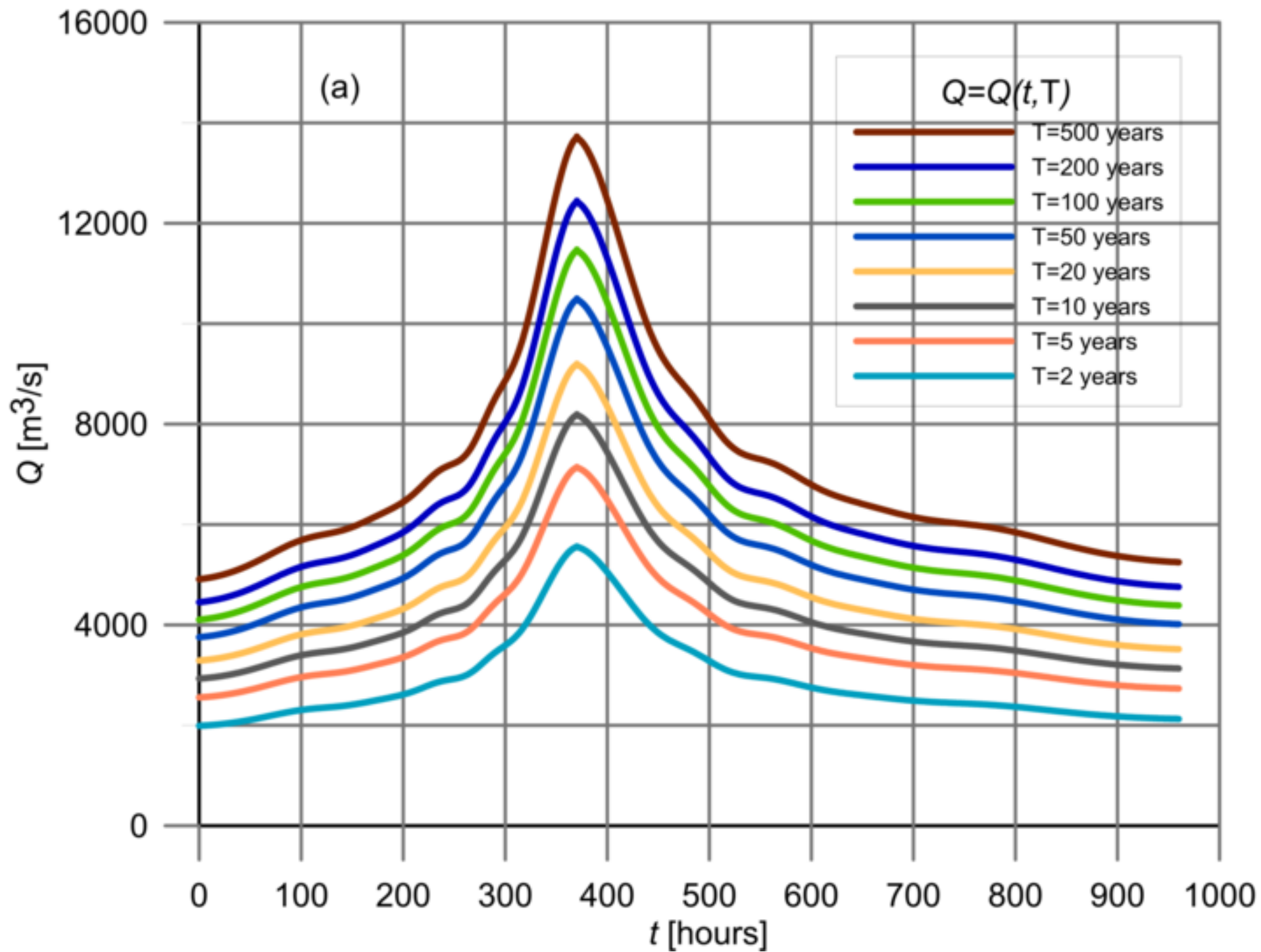


Figure 2b  
[Click here to download high resolution image](#)

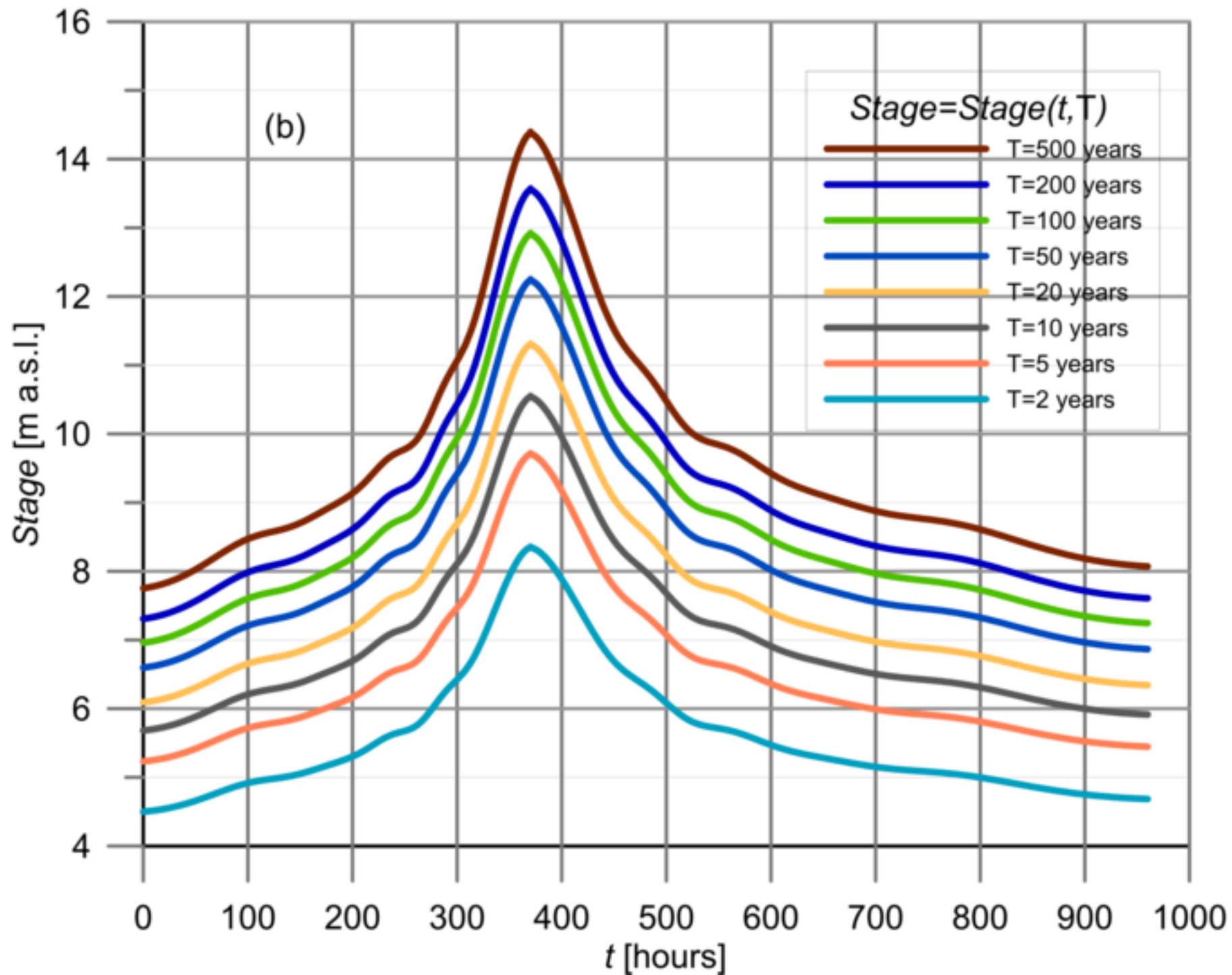


Figure 3  
[Click here to download high resolution image](#)

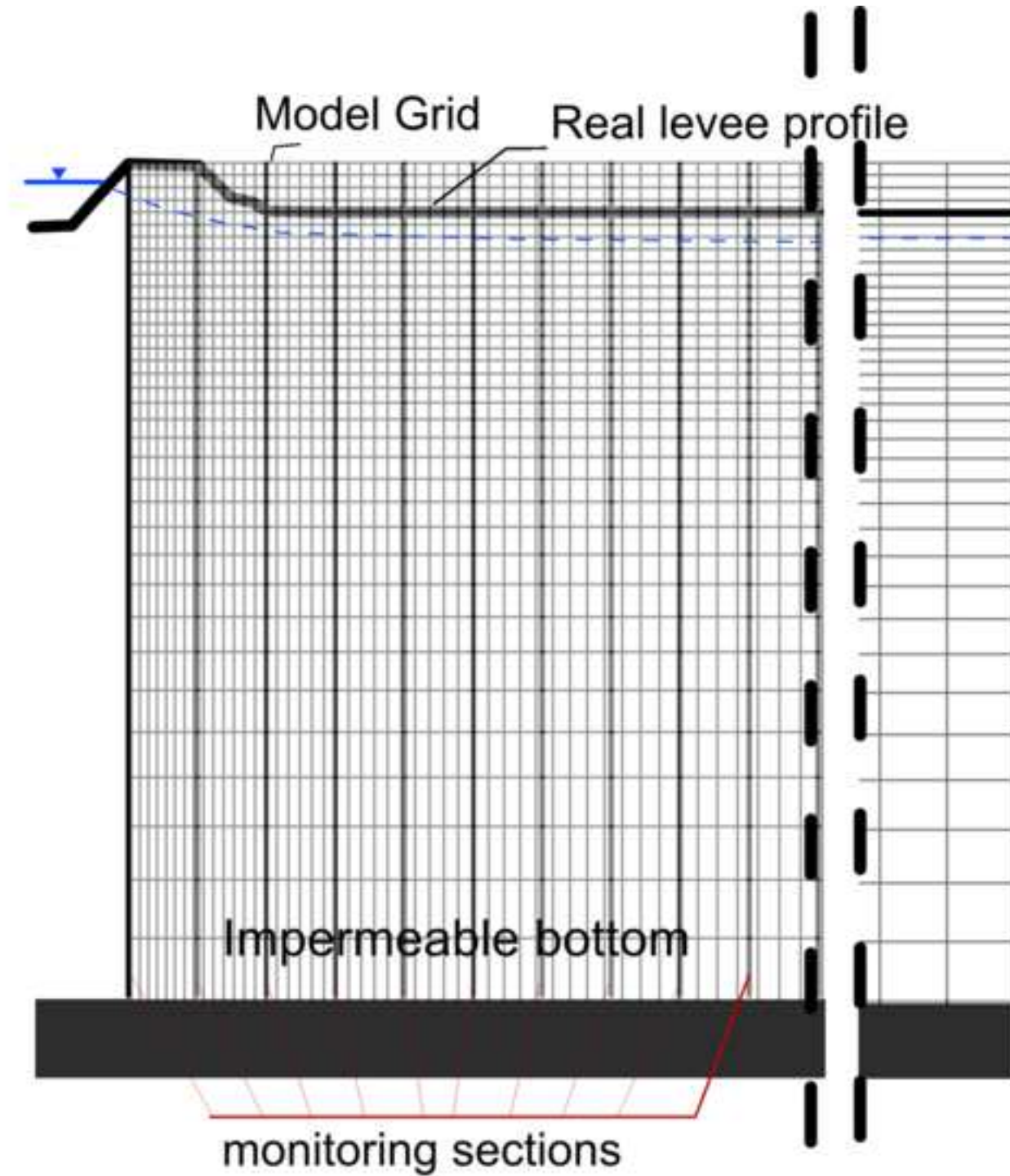
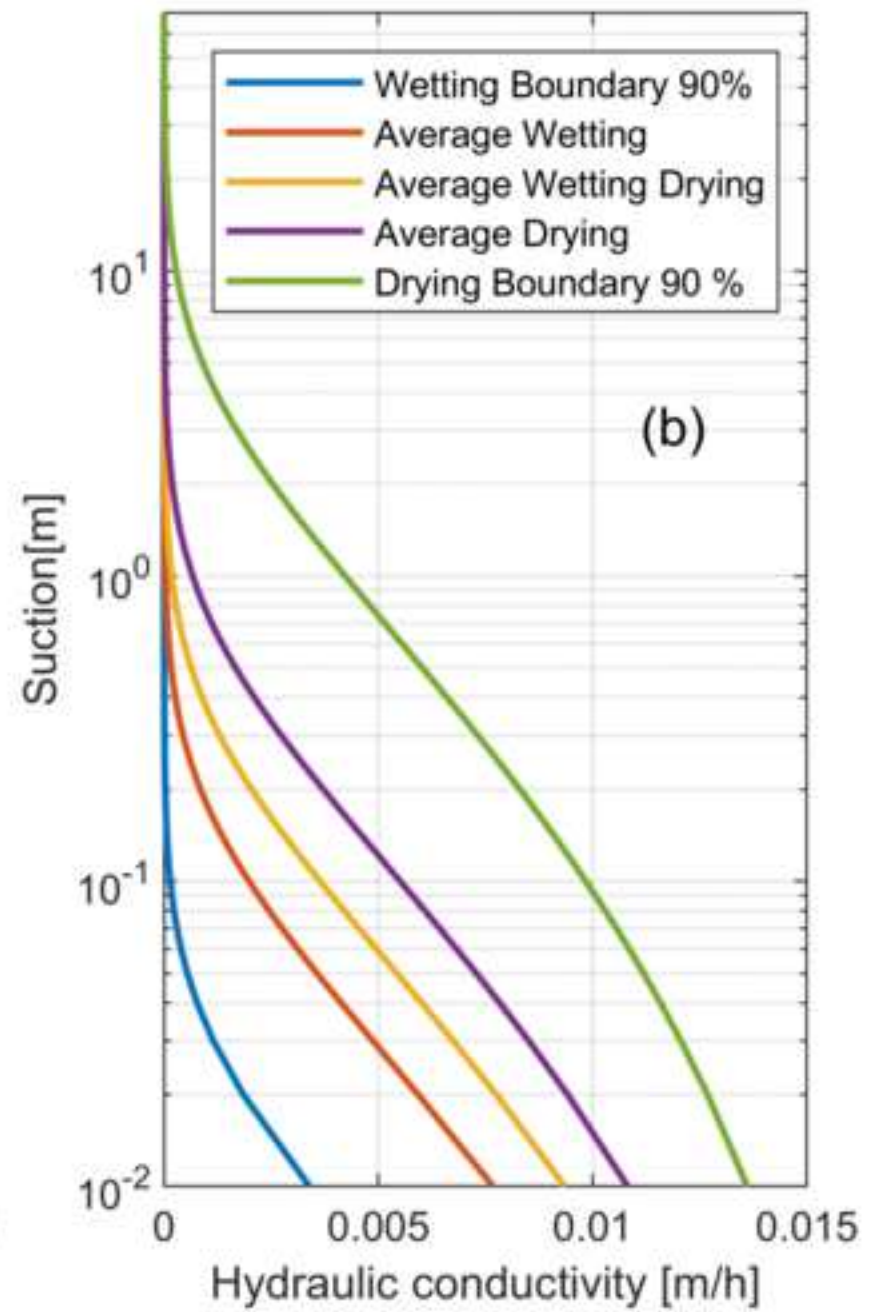
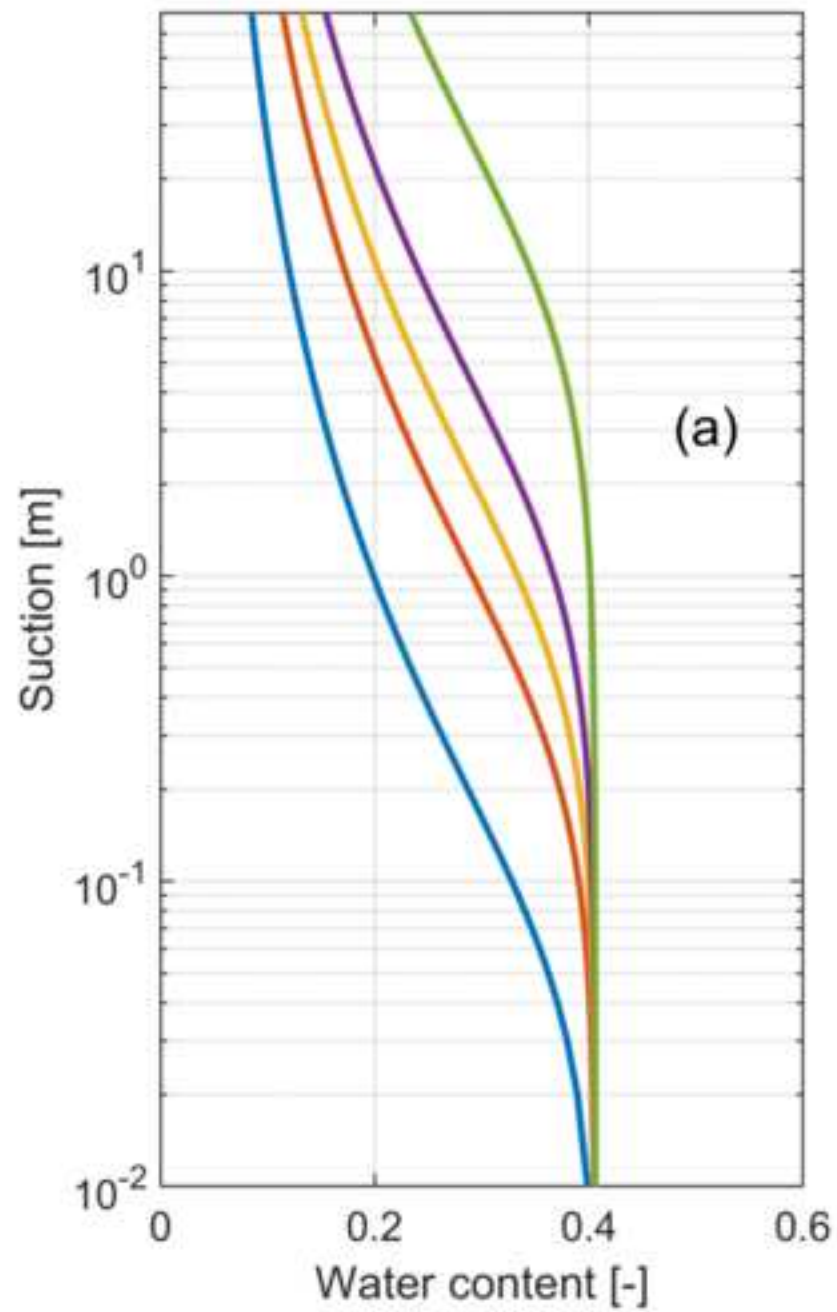


Figure 4  
[Click here to download high resolution image](#)





**Figure 5**  
[Click here to download high resolution image](#)

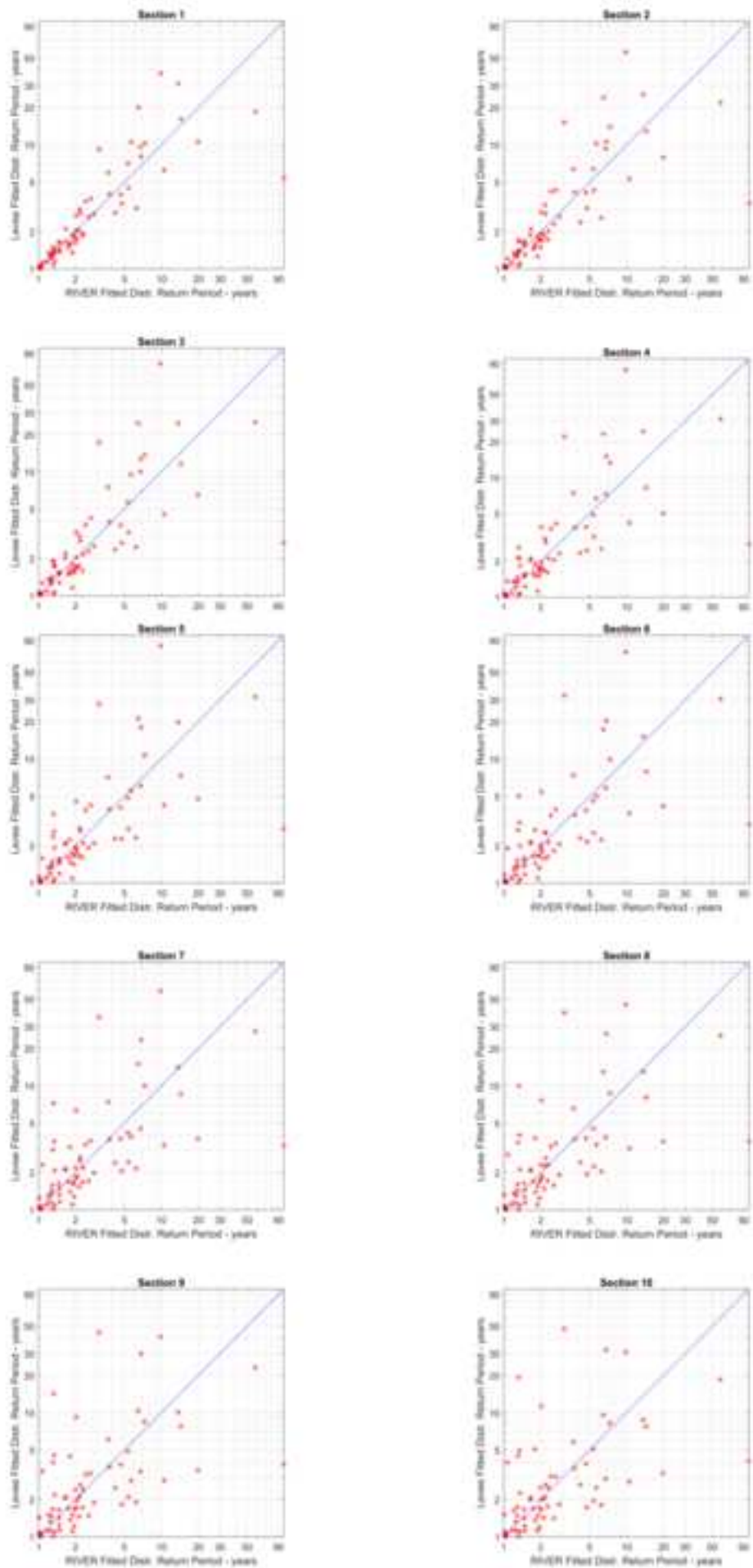


Figure 6  
[Click here to download high resolution image](#)

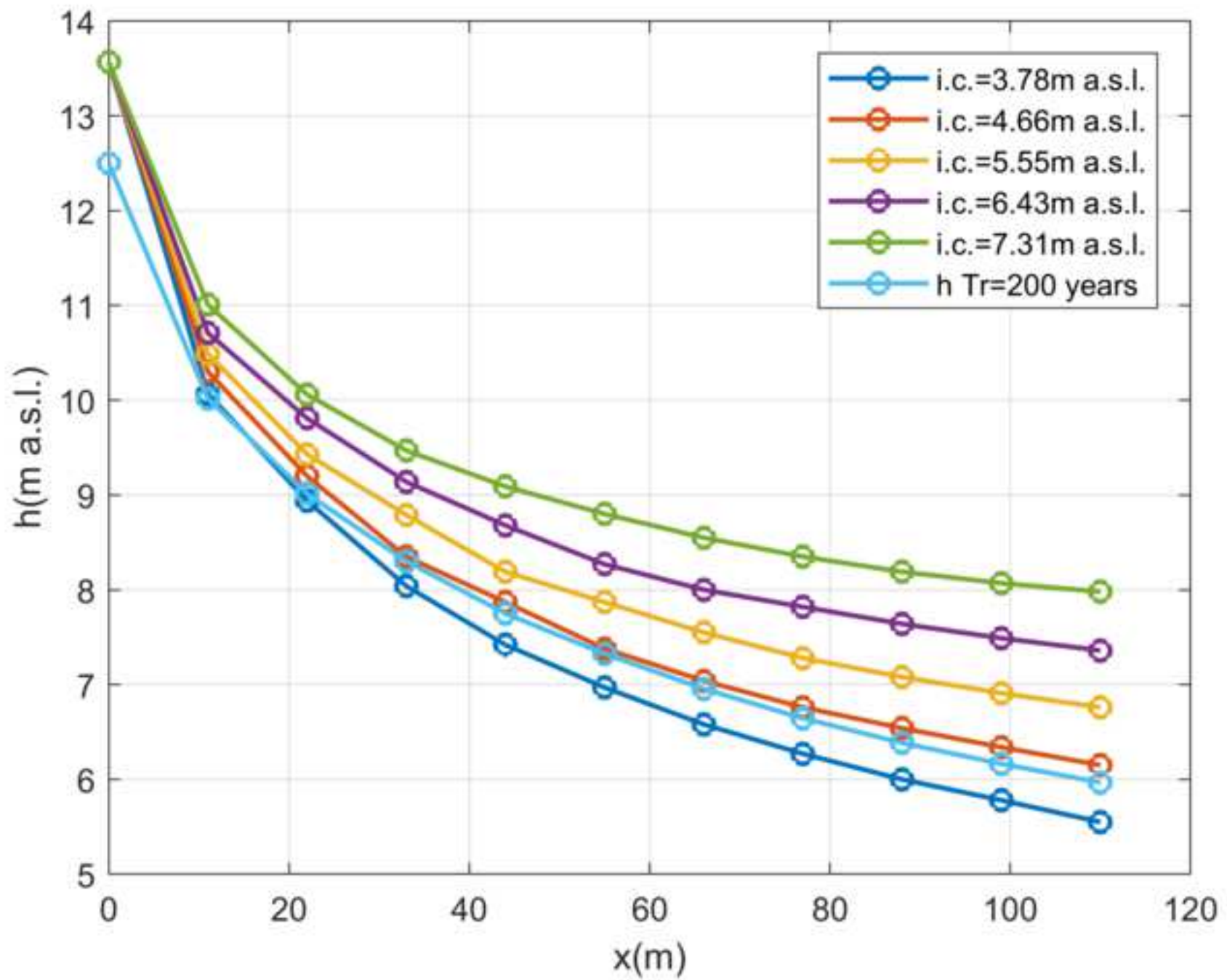
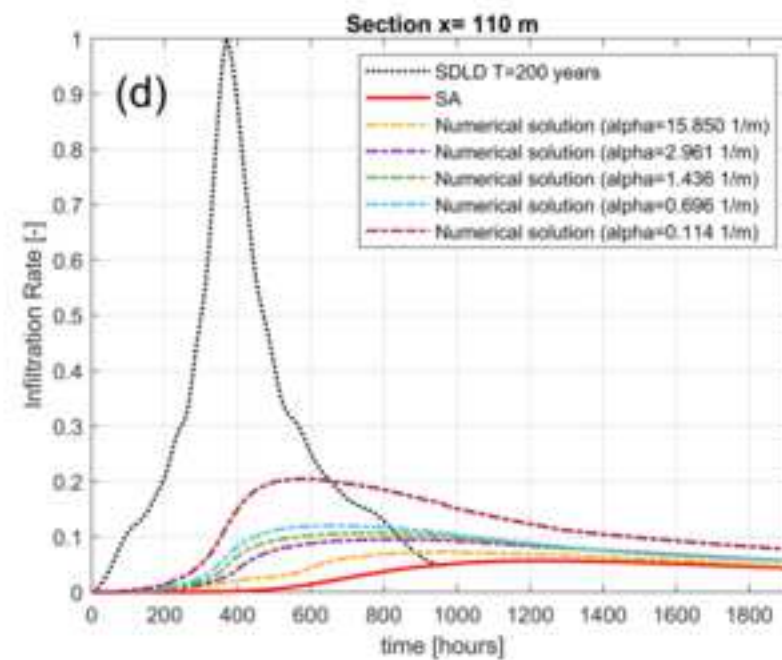
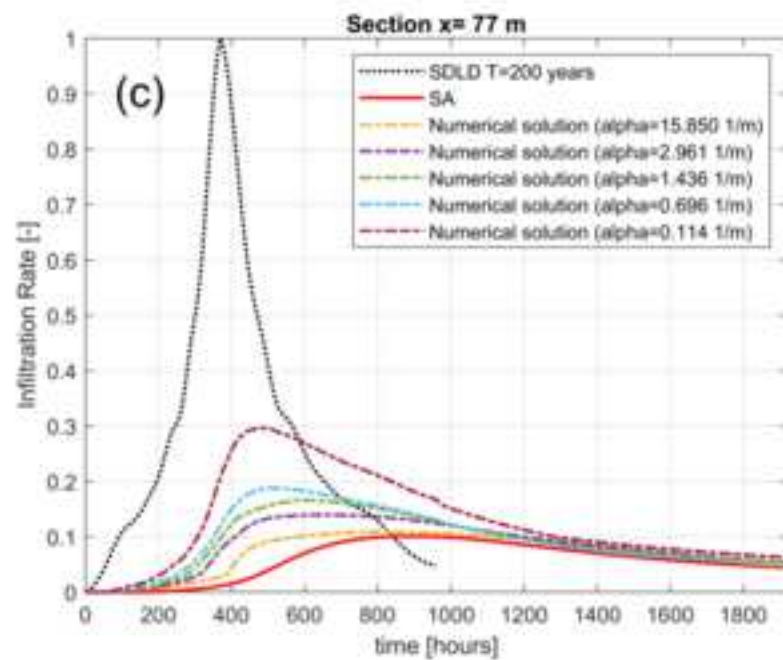
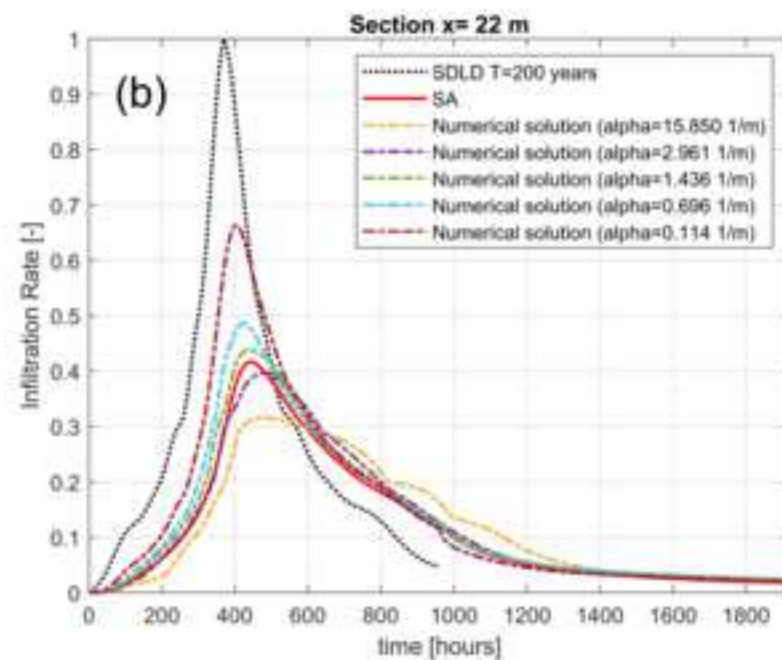
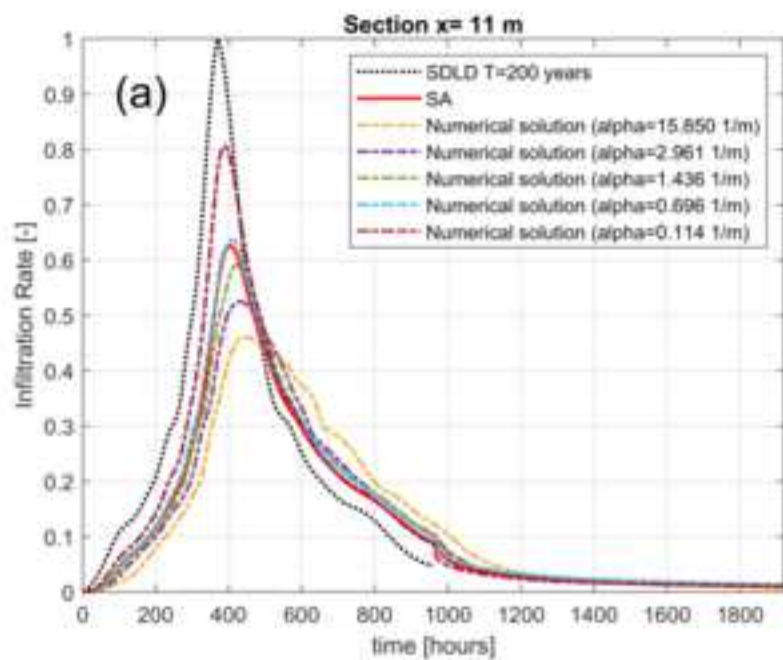


Figure 7  
[Click here to download high resolution image](#)



## Figure Captions

Figure 1. Stage duration curve at the Pontelagoscuro section of the Po River

Figure 2. Pontelagoscuro section: the Synthetic Design-Hydrographs for different return periods (a) and the Synthetic Design Level Diagrams derived from the SDH for a given return period (b).

Figure 3. The used mesh in the  $[xz]$  plane

Figure 4. The soil water retention curve (a) and the hydraulic conductivity versus suction curve (b) for the considered soil.

Figure 5. Return period (years) of the maximum yearly piezometric levels as a function of the flood return period at different distances from the riverside.

Figure 6. Maximum water levels reached in the levee using  $SDH_{1200}$  (labeled for  $T_r=200$  years), for different initial conditions of the piezometric levels, compared with the  $T_r=200$  year piezometric levels.

Figure 7.  $IR$  results obtained from numerical modeling compared with those obtained from the semi-analytical solution, for different values of the  $\alpha$  parameter and different distances from the river. (SDLD, derived from SDH for a return period equal to 200 years, as the river boundary condition).

Figure 8. Comparison of the piezometric levels obtained for different values of the  $\alpha$  parameter and different distances from the river. Results of the numerical simulations and semi-analytical model.

Table 1. Distance  $-x-$  of the observation sections in the levee from the riverside.

| <b>Location of the observation sections in the levee</b> |         |                |         |
|--|---------|----------------|---------|
| Section number   | $x$ [m] | Section number | $x$ [m] |
| 0  | 0       | 6              | 66      |
| 1  | 11      | 7              | 77      |
| 2  | 22      | 8              | 88      |
| 3  | 33      | 9              | 99      |
| 4  | 44      | 10             | 110     |
| 5  | 55      |                |         |

Table 2. Values of the unsaturated zone parameters.

| <i>Unsaturated zone parameter values</i>          | $\alpha$ [1/meter] | $n$ [-] | $m$ [-] |
|---|--------------------|---------|---------|
| Wetting Boundary 90 % confidence condition (WB90) | 15.850             | 1.3005  | 0.2311  |
| Average Wetting condition (AW)                    | 2.961              | 1.3005  | 0.2311  |
| Average Wetting-Drying (AW-D) condition           | 1.436              | 1.3005  | 0.2311  |
| Average Drying(AD) condition                      | 0.696              | 1.3005  | 0.2311  |
| Drying Boundary 90 % confidence (DB90) condition  | 0.114              | 1.3005  | 0.2311  |

Table 3. Maximum piezometric levels (m a.s.l.) reached at different distance from the river using different approaches to model the unsaturated zone.

| x(m) | S.A.                          | $\alpha=15.850$ 1/m<br>(WB90) | $\alpha=2.961$ 1/m<br>(AW) | $\alpha= 1.436$ 1/m<br>(AW-D) | $\alpha=0.696$ 1/m<br>(AD) | $\alpha=0.114$ 1/m<br>(DB90%) | Range of level<br>variations (m) |
|------|-------------------------------|-------------------------------|----------------------------|-------------------------------|----------------------------|-------------------------------|----------------------------------|
|      | piezometric levels - m a.s.l. |                               |                            |                               |                            |                               |                                  |
| 0    | 13.57                         | 13.57                         | 13.57                      | 13.57                         | 13.57                      | 13.57                         | ----                             |
| 11   | 11.23                         | 10.19                         | 10.6                       | 11.01                         | 11.3                       | 12.36                         | 2.17                             |
| 22   | 9.92                          | 9.29                          | 9.8                        | 10.06                         | 10.36                      | 11.46                         | 2.17                             |
| 33   | 9.13                          | 8.88                          | 9.21                       | 9.47                          | 9.8                        | 10.77                         | 1.89                             |
| 44   | 8.64                          | 8.43                          | 8.92                       | 9.09                          | 9.3                        | 10.23                         | 1.80                             |
| 55   | 8.32                          | 8.25                          | 8.61                       | 8.8                           | 8.96                       | 9.79                          | 1.54                             |
| 66   | 8.1                           | 8.11                          | 8.35                       | 8.55                          | 8.7                        | 9.44                          | 1.34                             |
| 77   | 7.94                          | 7.99                          | 8.18                       | 8.35                          | 8.49                       | 9.17                          | 1.13                             |
| 88   | 7.83                          | 7.91                          | 8.07                       | 8.19                          | 8.31                       | 8.94                          | 1.11                             |
| 99   | 7.74                          | 7.84                          | 7.98                       | 8.07                          | 8.17                       | 8.74                          | 1.00                             |
| 110  | 7.67                          | 7.76                          | 7.91                       | 7.98                          | 8.06                       | 8.59                          | 0.92                             |